

Efficient Channel Estimation With Optimization Algorithm-Based Pilot Pattern Design For MIMO-OFDM Wireless Networks.

Swetha Rani.L, Suriya Tarnnum

Abstract- In multiple input multiple output orthogonal frequency division multiplexing (MIMO-OFDM) frameworks, the channel state data ought to be known by the beneficiary for acquiring transmitted information. Channel estimation algorithms are utilized to look at the multipath effects of frequency selective Rayleigh blurring channels. It acquires the required channel data ahead of time with the aim of making the piloting code of the transmitter progressively proficient to influence the receiver to detect signals more effectively. In this way, the precision of channel estimation is the most critical in the concerns that determine the overall performance of a MIMO-OFDM system. In this paper, proficient channel estimation with optimization algorithm based pilot pattern design (ECE-OA) is proposed for MIMO-OFDM remote systems. It is utilized to reproduce the signal with improved spectral efficiency and requires transmitting the known pilot information to the receiver for estimating channel data. The ideal pilot patterns selected through reduce the negative effect of pilot pattern design. In ECE-OA, a chaotic social spider optimization (CSSO) algorithm is utilized to co-ordinate the assignment of pilot sequences across all cells to reduce the correlation between the pilots as observed at each base station. The multiple metrics are obtained from the uplink (UL) channel state information (CSI), during every UL period users in each cell transmit known pilot sequences to the base station in their own cells and the BS estimates uplink CSI. The proposed design used to maximize the accuracy of channel estimation and to reduce the computational complexity. The simulation results show that the performance of proposed ECE-OA design is perform better than existing state-of-art techniques in terms of bit error rate (BER) and Mean Square Error (MER).

Index Terms:Multi Objective Problem, Optimization Algorithm, Pilot decontamination, Multi factor social spilder optimization.

I. INTRODUCTION

MIMO technology has been shown to provide higher data rates with increased phantom proficiency [1][2]. The execution of a MIMO framework is straightforwardly identified with the gotten SINR and the relationship properties that are normal for the multipath channel and reception apparatus arrangement [3]. Despite the fact that the remote channel can convey low SINR at a portion of the MIMO get receiving wires, it is conceivable to improve framework execution with the utilization of beam forming at the transmitter. Despite the fact that regularly utilized together, it is imperative to separate here that beam forming is a flag preparing method, which is altogether different from shaft controlling where the bearing of the primary flap of radiation is changed. In MIMO, there are different receiving wires and utilized for synchronous transmission just as gathering. MIMO has the favorable position because of different reception apparatuses and propelled flag handling strategy utilized. By utilizing this procedure, different quantities of information streams can be transmitted or got over the MIMO reception apparatuses autonomously [4]. The impedance presented by the adjacent reception apparatuses is the principle issue of the MIMO system. Most MIMO plans are intended to accomplish only one of two accessible additions from these frameworks, are spatial multiplexing increase, spatial assorted variety gain [5]. There is, exchange off a tradeoff between otherworldly effectiveness and decent variety increase can be normal while considering MIMO usage. In any case, none of them recommended reasonable structures fit for accomplishing an ideal exchange off between spatial multiplexing and assorted variety gains [6]. Cross breed recognition in MIMO [7] emerges as answer for mutually accomplish spatial multiplexing and assorted variety gains. It is conceivable to significantly build the information rate while keeping a tasteful connection quality as far as bit mistake rate (BER) or SER [8]. Truth be

told, HMS apply unadulterated decent variety conspires together with unadulterated spatial multiplexing plans, so parts of the information are space-time coded over certain radio wires, and these parts are consolidated in layers.

The main challenge of hybrid detection in MIMO is to design a low-unpredictability, low-control, superior and high-throughput in equipment stage [9]-[12]. A few models have been proposed so far to address the issue, offering diverse tradeoffs among multifaceted nature and execution. Among them, ML identification [13] is the ideal recognition strategy and limits the BER through comprehensive hunt, despite the fact that its intricacy increments exponentially with the quantity of transmit and get radio wires. Then again, direct finders, for example, zero-compelling (ZF) [13][14], the MMSE [15] has lower intricacy with huge execution misfortune. Consequently an expansive class of identifiers has been proposed exchanging off among intricacy and execution misfortune, out of which the profundity first and expansiveness first inquiry calculations are very much assessed techniques. The profundity first strategy like SD [16] gives need to the drop hubs amid hunt procedure and follows back while coming to the leaf hubs. Despite what might be expected, the expansiveness first plan, for example, K-best identifier [17] considers a set number of hopefuls at each phase so as to continue to the following stage. The discovery calculation utilizes an early-pruned procedure that lessens the hub expansions in the K-Best circle decoder [18] while keeping up a practically greatest probability execution. For example, for 16-QAM is picked to be 5 while for 64-QAM, implying that the group of stars quadruples yet the K esteem just duplicates, along these lines the sub-straight increment [19]. It likewise has fixed basic way defer autonomous of the group of stars request, esteem, and the quantity of receiving wires. An arranging free K-best calculation for example dispersed K-best (DKB) and SIC [20] is utilized to diminish computational unpredictability.

For further enhancement, new channel estimation with optimization algorithm based pilot pattern design (ECE-OA) is proposed for MIMO-OFDM wireless networks. The proposed ECE-OA design is used to reconstruct signal with improved spectral efficiency and requires transmitting the known pilot data to the receiver for estimating channel information. The organization of this paper is as follows. The MIMO-OFDM design is reviewed in Section 2. In Section 3, we describe the problem methodology and system model of proposed design. The detailed description of proposed ECE-OA design is given in Section 4. Section 5 shows the simulation result comparison with other designs. Finally, the paper is concluded in Section 6.

II. RELATED WORKS

Huang et al. [21] have introduced an equipment productive engineering for 4×4 and 8×8 high-throughput MIMO indicators. The received non-consistent K-best calculation will in general keep more survival hubs in top hunt tree layers and decrease computational unpredictability in base layers rather than the regular K-best calculation. A pipelined design is utilized to produce one recognition yield for every clock cycle, in this manner meeting multi-gigabit throughput prerequisites for cutting edge remote correspondence frameworks. The productive collapsing plan strikes an appropriate harmony among unpredictability and throughput. The 4×4 indicator IC has 232kilogates equipment use. Its greatest estimated throughput is 4.08Gbps at 170-MHz working recurrence and 1.3-V center voltage.

Khairy et al. [22] have presented the calculation and engineering of a blunder flexible K-Best MIMO indicator dependent on the consolidated conveyance of channel clamor and instigated mistakes. The calculation depends on a youngster hub identification methodology amid the tree seeking and can significantly decrease the hunt space. The improvement techniques used to diminish the intricacy of the identifier and it integrated, set and steered to affirm the legitimacy and effectiveness. This calculation gives up-to 4.5 dB increase to accomplish the close ideal packet error rate (PER) execution in the 64-QAM framework. It flexible memory and accomplish up to 32.64% funds contrasted with the traditional K-Best identifier with immaculate memory.

Yan et al. [23] have proposed an adaptable double mode delicate yield MIMO identifier, which bolster open-circle and shut circle in Chinese EUHT remote neighborhood (LAN) standard. This indicator utilizes MMSE arranged QR disintegration (MMSE-SQRD) to create channel preprocessing result, which is acknowledged by an adjusted systolic exhibit engineering with simultaneous arranging. The received square-pull MMSE calculation for shut circle reuses MMSE-SQRD preprocessing to a great extent spare equipment overhead. An upgraded K-Best discovery calculation is utilized for open-circle, which expands throughput by odd-even parallel arranging and delivers high caliber delicate yield with disposed of ways. The MMSE-SQRD locator is executed in

SMIC 65 nm CMOS innovation and it equipped for running at 550 MHz, which has a greatest throughput of 2.64-Gbps for K-Best identification and 3.3-Gbps for straight MMSE discovery.

Faraji et al. [24] have proposed an effective fixed-point acknowledgment of an addition based delicate yield MMSE MIMO locator for LTE-A helpful remote correspondences. The dynamic scope of the transitional qualities in the identification calculation is improved utilizing the dynamic scaling plan. A range/accuracy estimation method is additionally utilized for ideal word-length extraction and the created fixed-point calculation is depicted and executed utilizing a word-length of 20 bits. This identifier is actualized on a Xilinx Virtex-7 FPGA accomplishing a most extreme clock recurrence of 422MHz. The throughput of this identifier surpasses 1146 Mbps and the inactivity is 0.6 μ s.

Sheikh et al. [25] have introduced a one of a kind methodology for MIMO identification that utilizes channel data to adjust the inquiry sweep of a K-best SD indicator. The assessed vitality decrease through recreations ranges from 10 to 51 %, contingent upon target BER and channel SNR. Amid troublesome SNR channel conditions, the MIMO indicator fulfills the objective BER by working at K= 5. At the point when channel SNR is high, 22nm circuit reenactments exhibit 68% decrease in vitality per-bit by setting K=1, while keeping up target BER. The channel versatile MIMO locator accomplishes 3.2Gbps throughput at an objective recurrence of 1.0GHz at 0.80 V supply and disperses most extreme 44.7pJ/piece.

Hsu et al. [26] have exhibited a configurable and versatile MIMO recognition framework dependent on the multi-center stage where the calculation hubs are interconnected utilizing the Network-on-Chip (NOC) worldview. A tree-seeking based MIMO location calculation is overhauled to be appropriate for the NOC framework, and the handling components that execute the calculation is architected. The mapping strategy of the calculation onto the NOC stage is utilized to play out the whole MIMO identification conspires. The two sorts of NOC topologies are executed so as to clarify the structure exchange offs between the preparing speed and the framework multifaceted nature. This MIMO identification plot is profoundly configurable to help distinctive framework arrangements including number of reception apparatuses and tweak conspires, and is reasonable for substantial scale MIMO framework that outfits with extensive number of radio wires.

Peng et al. [27] have proposed a parallelizable Chebyshev cycle (PCI), which lessens the figuring load and investigates the potential parallelism of lattice reversals and duplications. An eigenvalue-estimate based technique is utilized to get an underlying arrangement and Chebyshev cycle is connected for the surmised calculation of grid reversals and augmentations. The PCI strategy disposes of the connections in extensive scale lattice reversals and augmentations, in this way improving the parallelism among components of the evaluated vector. These enhancements are accomplished at the expense of a minor decrease in location precision. In view of the PCI technique, a completely pipelined design with normal handling components is utilized to acknowledge 64-QAM MMSE recognition. The iterative parameters are gotten through estimated calculations and are utilized over and again, and the client level pipeline handling design accomplishes an ideal exchange off among the throughput, region and power utilization.

Fan et al. [28] have introduced a two-dimensional parallel arranging calculation for high-throughput K-best indicators used in MIMO frameworks. The arranging calculation improves the throughput by arranging an informational index in parallel and dodges the generally long inertness of the customary calculations. This is particularly significant in MIMO frameworks using high-request tweak plans. They utilized the arranging calculation in a K-best locator with variable K esteems at various layers of the hunt tree, which improves the BER execution and lessens the computational intricacy. The finder utilizing the arranging calculation is planned and executed in TSMC 90-nm CMOS innovation for 4×4 64-QAM MIMO frameworks.

Liu et al. [29] have proposed a client level parallelism-based completely pipelined engineering for a MMSE finder for an uplink 128×8 64-QAM gigantic MIMO framework. A corner to corner based systolic exhibit with single-sided input is received with this plan, which wipes out the throughput constraint. A weighted Jacobi-emphasis based design is utilized to iteratively accomplish grid reversal, subsequently decreasing the computational burden and misusing the potential parallelism of the lattice reversal. An approximated engineering is utilized to register the log-probability proportion. Tseng et al. [30] have exhibited a high-throughput multi-mode preprocessor for 4×4 MIMO finder utilizing numerous pre-preparing plans including QR disintegration (QRD), Sorted QRD (SQRD), or MMSE-SQRD. So as to accomplish high preparing throughput, this configurable pre-processor is architected dependent on the Givens pivot calculation and a pipelined systolic cluster structure. Also decreasing the equipment intricacy and mitigating overhead for configurability, a few plan developments have been connected. A standard computation plot is used to limit the arranging tasks and used circuit components are structured considering the equipment sharing ideal models.

III. Problem definition and system model

A. Problem methodology

Xiao et al. [31] have designed pilot designs by limiting the shared lucidness of the estimation lattice with the GSIP. At that point two pilot design configuration plans named pilot structure with GSIP (PDGSIP) and tradeoff pilot structure with GSIP (TPDGSIP) are advanced to structure symmetrical pilot designs dependent on GSIP for a MIMO-OFDM framework. In PDGSIP, a gathering of pilot designs are initially gotten and after that pilot designs having vast shared intelligence are supplanted with new ones produced with ideal pilot designs. TPDGSIP legitimately delivers new pilot designs dependent on GSIP to completely misuse the pilot separation of the acquired pilot design when one pilot design is gotten. This pilot design configuration plans can get the best pilot designs in contrast with existing strategies from the point of view of common lucidness

Dissimilar to many existing plans, the proposed technique does not require data trade among the BSs or earlier data about the channels of all cells. The UL information access from the objective cell and after that acquires the LS channel gauge by regarding the distinguished UL information as pilot images. The UL information from various clients in the objective cell is assessed successively. For every user, gathering obliged minimization issue utilizing an offbeat pilot protocol and the optimization calculation used to take care of those issues. From optimization calculation process the coveted information source from watched mixture signal. The semi-blind based pilot decontamination strategy diminish the information length develops but authors not focusing optimization part. To overcome those problems, efficient channel estimation with optimization algorithm based pilot pattern design (ECE-OA) is proposed. The main objective of proposed ECE-OA design is summarized as follows:

- In ECE-OA, a chaotic social spider optimization (CSSO) algorithm is used to co-ordinate the assignment of pilot sequences across all cells to reduce the correlation between the pilots as observed at each base station.
- The multiple metrics are obtained from the uplink (UL) channel state information (CSI), during every UL period users in each cell transmit known pilot sequences to the base station in their own cells and the BS estimates uplink CSI.
- ECE-OA design used to maximize the accuracy of channel estimation and to reduce the computational complexity.
- The simulation results show that the performance of proposed ECE-OA design is perform better than existing state-of-art techniques in terms of bit error rate (BER) and Mean Square Error (MER).

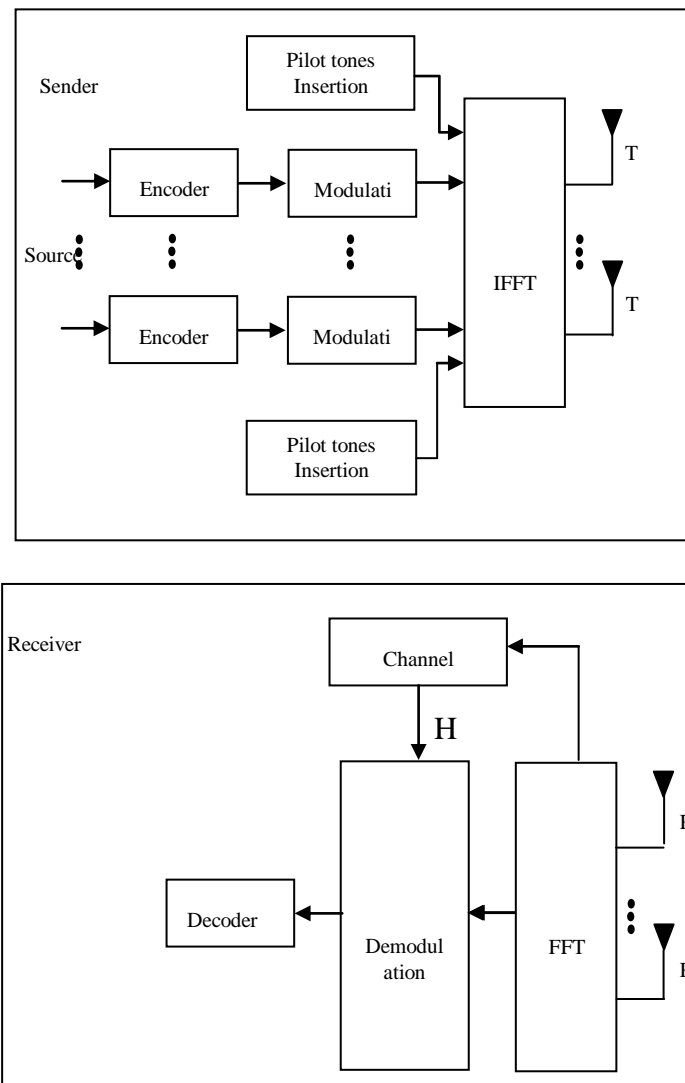


Fig. 1. MIMO-OFDM system with proposed ECE-OA design

Figure 1 demonstrates the framework model of proposed effective channel estimation with improvement calculation based pilot design plan (ECE-OA). At the sender side, the encoded information streams might be regulated utilizing distinctive heavenly body sets of QAM images. At that point, a IFFT is performed to encode the information on different bearer frequencies. When the collector has procured the flag it is changed utilizing FFT. The channels exchange work H is evaluated to be encouraging the flag discovery, which recuperates the transmitted image given H and the got image. The utilization of different transmit channels permits the MIMO-OFDM framework to maximally utilize restricted range and convey information at high rates. MIMO finder consolidates every complex got motion before further preparing in the channel decoder. At last the channel decoder reestablishes the bit data sent from the source.

A spatial multiplexing MIMO system with 'T' number of transmits antennas and 'R' number of receive antennas is represented as follows:

$$y = Hx + N \quad (1)$$

Where x is the complex transmitted symbol vector i.e. $x = (x_1, x_2, \dots, x_T)^T$ and each element is independently drawn from complex constellation S of M-QAM order. $y = (y_1, y_2, \dots, y_R)^T$ is the complex received symbol, H is equivalent baseband model of the Rayleigh fading channel between the transmitter and the receiver and is defined by $R \times T$ dimensional complex channel matrix and N is assumed to be additive white Gaussian noise (AWGN) vector with zero mean and covariance matrix

Encoder/Decoder is a generalized form of Alamouti method, which are symmetrical and can accomplish transmit assorted variety distinguish by the more number of transmit reception apparatuses. The space-time square codes are a composite technique for Alamouti space-time code, where the encoding and unraveling strategy are equivalent to there in the Alamouti space-time code on both the transmitter and recipient sides. At the recipient side, the signs got are first bring together and after that send to our NHMD where the assurance rules are executed. Space-time square codes were produce to do the most extreme assorted variety request for the given progressively number of transmit and get radio wires subject to the control of having a straightforward direct disentangling method.

Modulation/Demodulation schemes are the distinct building blocks in digital communication system. Digital data is represented by exhaustible number of digital signals and it has finite number of periods and each periods are encodes in equal number of digital bits. QAM techniques can be extending to implement the modulation and demodulation schemes. The low power QAM modulator and demodulator are expound by consider the data values inside the memory as per the design data. An assortment of types of QAM are accessible and a portion of the more typical structures incorporate 16 QAM, 32 QAM, 64 QAM, 128 QAM, and 256 QAM. Here the figures allude to the quantity of focuses on the heavenly body, for example the quantity of particular expresses that can exist. While it is conceivable to transmit more bits per image, if the vitality of the heavenly body is to continue as before, the focuses on the group of stars must be nearer together and the transmission turns out to be progressively defenseless to clamor. This outcomes in a higher BER than for the lower request QAM variations. Along these lines there is a harmony between getting the higher information rates and keeping up a satisfactory piece blunder rate for any radio correspondences framework.

The FFT work as pursues:

$$X(\omega) = \sum_{\phi=0}^{M-1} x(\phi) W_M^{\phi\omega}; \quad \omega = 0, 1, \dots, M-1 \quad (2)$$

where $W_M^{\phi\omega}$ is twiddle factor,

$$W_M^{\phi\omega} = e^{-j(2\pi/M)} \quad (3)$$

Similarly, IFFT function as follows:

$$x(\phi) = \frac{1}{M} \sum_{\omega=0}^{M-1} X(\omega) W_M^{-\phi\omega}; \quad \phi = 0, 1, \dots, M-1 \quad (4)$$

FFT design consists of four stages.

IV. Pilot Pattern Design Using Efficient Channel Estimation with Optimization Algorithm

In proposed ECE-OA design, first to estimate the channel to improve the unearthy effectiveness and requires transmitting the known pilot information to the collector. Then constraints for optimal pilot sequence assignment and the working function of CSSO algorithm are discussed in the following section.

A. Channel estimation MIMO-OFDM

At the receiver side, due to the phase difference effects of received signal causes multipath fading. It occurred due to the received signals travelled in different distances and paths. The Rayleigh distributions are used which reaches at a receiver by more than one path. Rayleigh distribution is most normally used for fast fading case. The probability density function of Rayleigh distribution is,

$$F_{Ray} = \frac{r}{\sigma^2} e^{-r^2/\sigma^2}; \quad r \geq 0 \quad (5)$$

where r is the random variable and σ^2 is the variance. AWGN channel is common channel representation for verifying all modulation techniques. Here the white Gaussian noise to signal passing all the way through it, because it is known that it has uniform power across the frequency band for overall system.

$\hat{j}_n^{p,q} = [j_{p,q}(0,n), \dots, j_{p,q}(Q-1,n)]^T$, $0 \leq n \leq N-1$, where $j_n^{p,q}$ signifies the nonzero components of the n th line in the time area channel grid $D_{p,q}$ as shown below:

$$D_{p,q} = \begin{bmatrix} j_{p,q}(0,0) & 0 & \dots & j_{p,q}(2,0) & j_{p,q}(1,0) \\ j_{p,q}(1,1) & j_{p,q}(0,1) & \dots & j_{p,q}(3,1) & j_{p,q}(2,1) \\ \vdots & \vdots & & \vdots & \vdots \\ 0 & 0 & \dots & j_{p,q}(0,N-2) & 0 \\ 0 & 0 & \dots & j_{p,q}(1,N-1) & j_{p,q}(0,N-1) \end{bmatrix}$$

Each column of $D_{p,q}$ has L non-zero components. Here, time-space lattice $D_{p,q}$ is parameterized, by utilizing few its columns, which is spoken to by R . This puts R markers physically in the time space in which the channel coefficients are determined. From that point forward, the channel coefficients at different occasions are interjected by using these time-area markers. This thought limits the quantity of parameter to be registered from NL to RL , where $R \ll N$. Subsequently, we initially select R columns of $D_{p,q}$, which are represented by $j_{r(1)}^{p,q}, \dots, j_{r(R)}^{p,q}$ as R markers for the time space marker in $D_{p,q}$. $R_{p,q} := [r(1), \dots, r(R)]$ is the arrangement of these line files of the time-space marker. Each channel $j_n^{p,q}$, where $n \in R_{p,q}$, can be communicated as a straight blend of these R markers $j_{r(1)}^{p,q}, \dots, j_{r(R)}^{p,q}$:

$$j_{p,q}(l,n) = b_{l,n,p,q}^T [j_{p,q}(l,r(1)), \dots, j_{p,q}(l,r(R))]^T \quad (7)$$

For $0 \leq l \leq L-1$ where

$$\mathbf{b}_{l,n,p,q} = [\mathbf{b}_{l,n,p,q}(r(1)), \dots, \mathbf{b}_{l,n,p,q}(r(R))]^T \quad (8)$$

is an $R \times 1$ vector of time-area introduction loads used to express the channel coefficient between P th transmit receiving wire and get reception apparatus at time n . For lessening the quantity of addition loads that is required to structure each channel coefficient and is communicated as $j_{p,q}(l, n)$ at time n as an addition between two time-space markers, comparable to the way at time $r(k)$ and $r(k')$, that is $j_{p,q}(l, r(k))$ and $j_{p,q}(l, r(k'))$, where $r(k), r(k') \in R_{p,q}$. The interpolation weight vector $\mathbf{b}_{l,n,p,q}$ in eq. (8) is improved to have just two non-zero components $\mathbf{b}_{l,n,p,q}(r(k))$ and $\mathbf{b}_{l,n,p,q}(r(k'))$. Thus, think about that the connection between $j_{p,q}(l, r)$ and $j_{p,q}(l, n)$ can be communicated as beneath:

$$H[r, n] := O[j_{p,q}(l, r) j_{p,q}^J(l, n)] \quad (9)$$

After that the estimation of the ideal introduction weight is direct. For this, first characterize $\tilde{j}_{n,p,q}(l) := [j_{p,q}(l, r(k)), j_{p,q}(l, r(k'))]$ as the arrangement of chose time-space marker used to mean the $j_{p,q}(l, n)$ and $\mathbf{b}_{l,n,p,q}^{NE} := [\mathbf{b}_{l,n,p,q}(m(k'))]^T$ as the arrangement of non-zero components of addition weight vector $\mathbf{b}_{l,n,p,q}$ relating to the components of $\tilde{j}_{n,p,q}(l)$. the arrangement of non-zero interjection weight $\mathbf{b}_{l,n,p,q}^{NE}$ that limits the channel estimation blunder is characterized as underneath:

$$O[\|\mathbf{j}_{p,q}(l, n) - \mathbf{b}_{l,n,p,q}^{NE} \tilde{j}_{n,p,q}^J(l)\|^2] \quad (10)$$

can be effectively acquired by utilizing symmetry standard as underneath

$$\mathbf{b}_{l,n,p,q}^{NE} \tilde{j}_{n,p,q}^J = \mathbf{A}_{n,j\tilde{j}}^{p,q} \mathbf{A}_{n,\tilde{j}\tilde{j}}^{p,q}{}^{-1} \quad (11)$$

where $\mathbf{A}_{n,j\tilde{j}}^{p,q} = O[\mathbf{j}_{p,q}(l, n) \tilde{j}_{n,p,q}^J(l)]$, and $\mathbf{A}_{n,\tilde{j}\tilde{j}}^{p,q} = O[\tilde{j}_{n,p,q}(l, n) \tilde{j}_{n,p,q}^J(l)]$

Consequently, following outcome can be gotten:

$$\mathbf{A}_{n,j\tilde{j}}^{p,q} = [H[r(k), n], H[r(k'), n]] \quad (12)$$

$$\mathbf{A}_{n,\tilde{j}\tilde{j}}^{p,q} = \begin{bmatrix} H[r(k), r(k)] & H[r(k), r(k')] \\ H[r(k'), r(k)] & H[r(k'), r(k')] \end{bmatrix} \quad (13)$$

It is essential to take note of that $b_{l,n,p,q}^{NE}$ relates to the non-zero components of $b_{l,n,p,q}$ in (12) now $r(k)$ and $r(k')$. Consequently, $b_{l,n,p,q}$ in (12) can be composed as underneath:

$$b_{l,n,p,q} = [0, \dots, 0, b_{l,n,p,q}(r(k')), 0, \dots, 0]^T \quad (14)$$

In channel estimation, gotten flag is recovered regarding the time-space markers. It is viewed as that in the t_{th} emphasis, the transmitted information image vector $V^{(t-1)}$, which is identified in the $(t-1)th$ cycle is presently accessible at the beneficiary

$$B_q(k) = \sum_{p=1}^{Y_T} \sum_{o=0}^{N-1L-1} \sum_{l=0}^Y \sum_{i=1}^Y a_{m(i)}^{k,p} (l) d_{p,q}(l, m(i)) U_p^{t-1}(o) + g_q(k) \dots \quad (15)$$

where $g_q(k)$ represents the summation of the estimation error at subcarrier k and AWGN at the q^{th} receive antenna, and

$$a_{m(i),p,q}^l(l) = \frac{1}{N} h_{o,l} \sum_{w=0}^{N-1} [B_{m(i)}^{p,q}]_{w,w} e^{\frac{2\pi j w(o-m)}{N}} \quad (16)$$

B. Constraints for Pilot sequence assignment

The multiple constraints used for the pilot sequence assignment are received signal strength, large scale fading, signal to interference plus noise ratio, pair-wise error probability and normalized mean square error.

C. Received signal strength (RSS)

The vitality utilization relies upon both transmitter and recipient vitality prerequisites. The vitality utilization of a client is relative to square of separation (D^2) when the spread separation (D) not exactly the limit remove (D_0), else it is corresponding to (D^2). The all out vitality utilization Of every client in the system for transmits and gets bit information parcel.

$$E_{total} = E_{tx}(n, d) + E_{rx}(n) \quad (17)$$

Where $E_{tx}(n, d)$ and $E_{rx}(n)$ are vitality utilization of transmitting and accepting client.

$$E_{tx}(n, d) = \begin{cases} n \times E_{elec} + n \times \epsilon_{fs} \times D^2; & \text{if } D < D_0 \\ n \times E_{elec} + n \times \epsilon_{mp} \times D^4; & \text{if } D \geq D_0 \end{cases} \quad (18)$$

$$E_{rx}(n) = n \times E_{elec} \quad (19)$$

where E_{elec} the vitality is dispersed per bit to run the transmitter or recipient circuit, intensification vitality with the expectation of complimentary space model (ε_{fs}) and for multi-way model (ε_{mp}) relies upon the transmitter intensifier model and D_0 is the limit transmission remove.

Received Signal Strength (RSS) is the direct normal of the all out vitality utilization watched just in OFDM images conveying reference images from all sources, including co-channel non-serving and serving cells, adjoining channel impedance and warm clamor. RSS is dictated by the separation and transmission vitality, if the client transmits parcel with vitality, $E_{tx}(n, d)$, the hubs got flag quality RSS, with the separation of D, can be communicated as pursues:

$$RSS = \frac{E_{tx}(n, d)}{4\pi D_i^2} + T_{a, a_1/a_2} \quad (20)$$

D. Large-scale fading

Because of the way loss of flag as a component of separation and shadowing by vast items makes extensive scale blurring. This happens as the versatile travels through a separation of the request of the phone measure and is regularly recurrence-free. Large scale fading describes variation in the local mean during a relative long observation. Consider a cell organize made out of L hexagonal cells. Every cell contains K single-reception apparatus clients and one BS outfitted with M radio wires. A similar recurrence band is utilized for all L cells and TDD mode is utilized. The UL transmission and accept that the channel is time-invariant amid the UL transmission. The large-scale fading can be expressed as follows [34]:

$$\beta = \begin{cases} \beta_{l,l,k} = 1; & \text{Pilot sequence request from same cell} \\ \beta_{l,i,k} = 0.3; & \text{Otherwise} \end{cases} \quad (27)$$

where $\beta_{l,l,k}$, $\beta_{l,i,k}$ is the extensive scale blurring coefficient between the k^{th} user in the l^{th} cell and the m^{th} antenna of the l^{th} BS and the i^{th} cell of the l^{th} BS respectively.

E. Signal to Interference Plus Noise Ratio (SINR)

SINR relies upon the quantity of radio wires and number of clients per base station develops huge while keeping up a fixed proportion and it is communicated as pursues [18]:

$$SINR = \frac{P_s}{\sigma^2 + \sigma \cdot P_{i-pc}} \quad (28)$$

where P_s is the signal power, P_{i-pc} is the obstruction control because of pilot pollution and σ the noise variance respectively.

F. Pair-wise Error Probability (PEP)

Give us initial a chance to expect that the considered framework just has two code words. Since the main BS is concerned, we accept that these two code words are as per the following:

$$C_i = (c_{1i}, c_{2i}, \dots, c_{ti})^T; \quad i = 1, 2 \quad (29)$$

where C_1 and C_2 are $1 \times t$ matrices. From the first BS's view, C_1 and C_2 have the most grounded closeness among all codeword combines, and are the most hardest to be recognized. The PEP can be communicated as pursues [19]:

$$PEP = P(C_1 \rightarrow C_2)p(C_1) + P(C_2 \rightarrow C_1)p(C_2) \quad (30)$$

where $P(C_a \rightarrow C_b)$, denotes the probability of decoding output C_b given that C_a is transmitted, and $p(C_a)$ is the probability of transmitting C_a .

E. NMSE

The NMSE might compute by the total pilot signal received, n^{th} signal acknowledged by the m^{th} projection in the l^{th} cell might be articulated as follows [34]:

$$Z_{l,m}(n) = \sqrt{E_{total}} \sum_{k=1}^K t_{l,l,m,k} x_{l,k}(n) + \sqrt{E_{total}} \sum_{i=1, i \neq l}^L \sum_{k=1}^K t_{l,i,m,k} x_{i,k}(n) + z_{l,m}(n) \quad (31)$$

Where, $1 \leq l \leq L$ & $1 \leq m \leq M$,

$\sqrt{E_{total}}$ has the total energy consumption of every operator, $x_{l,k}(n)$ is the n^{th} symbol conveyed by the k^{th} worker in the l^{th} cell $z_{l,m}(n)$ is composite Gaussian noise, $t_{l,l,m,k}$ is the channel coefficient between the k^{th} user in the l^{th} cell m^{th} antenna in the l^{th} BS is expressed as follows [34]:

$$t_{l,l,m,k} = \alpha_{l,l,m,k} \cdot \sqrt{\beta} \quad (32)$$

Where, $\alpha_{l,l,m,k}$ is the slight scale declining and β is the huge scale fading. Using the equations (27), (28), the

general received signal requests are modeled as follows [34]: $Z_l = \sqrt{E_{total}} T_{l,l} x_l + \sqrt{E_{total}} \sum_{i=1, i \neq l}^L T_{l,i} x_i + z_l$

(33)

Consider the first cell and the Z_l used to estimate the UL channel data i.e. $T_{l,l}$. The presentation with the station approximation is normally measured in relations with the NMSE, that can be distinct as follows:

$$NMSE = \frac{E \left\{ \left\| \hat{H}_{l,l} - H_{l,l} \right\|^2 \right\}}{E \left\{ \left\| H_{l,l} \right\|^2 \right\}} \quad (34)$$

where $\hat{H}_{l,l}$ is the estimate of $H_{l,l}$.

G. Pilot Pattern Design using Chaotic Social Spider Optimization (CSSO) Algorithm:

The CSSO procedure inspired from the swarm procedure and introduced in [35]. Encouraged by the communal spiders (SSA), authors at [34] modify the SSA to tackle worldwide streamlining issues. This calculation is primarily founded on the scrounging methodology of social bugs, using the vibrations on the bug catching network to decide the places of injured individual. This calculation imitates the conduct of social insects to perform streamlining. The arrangement of streamlining issue is the situation of creepy crawlies through insect hunting space that is mindful down interpreting the data between bugs. The correspondence between the creepy crawlies is performed utilizing vibration that transmitted when the insects move to another position. The vibration among creepy crawly and is produced by the weight and position of as pursues:

$$V_{a_{i,j}} = v_{a_j} e^{-d_{a_{i,j}}^2}; d_{a_{i,j}} = \|a_i - a_j\| \quad (35)$$

Where,

v_{a_j} is the weight of the spider a_j which is defined as follows

$$v_{a_j} = \frac{FF(a_j) - W_a}{B_a - W_a} \quad (36)$$

Where,

$FF(a_j)$ is the suitability purpose worth attained by assessment of a_j , and the W_a , B_a is the wickedest and finest case correspondingly as surveys:

$$W_a = \min_{k=1, \dots, K} FF(a_k) \quad (37)$$

$$B_a = \max_{k=1, \dots, K} FF(a_k) \quad (38)$$

There are two procedures to refresh the situation of insects relying upon their sexual orientation; where there are two sorts of sex, guys and females (the females speak to 60–90% from the absolute number of bugs). The female bug refreshes its situation as pursues:

$$X_{FM_{a_i}}^k = \begin{cases} X_{FM_{a_i}}^k + r_1 \times v_{a_i} \times (a_1 - X_{FM_{a_i}}^k) + r_2 \times v_{a_i} \times (a_2 - X_{FM_{a_i}}^k) + r_3 \times (\xi - 0.5) & \text{Random} \geq M \\ X_{FM_{a_i}}^k - r_1 \times v_{a_i} \times (a_1 - X_{FM_{a_i}}^k) - r_2 \times v_{a_i} \times (a_2 - X_{FM_{a_i}}^k) - r_3 \times (\xi - 0.5) & \text{Otherwise} \end{cases} \quad (39)$$

where r_1 , r_2 , r_3 , $Random$ and ξ are irregular numbers between (0, 1), while M is limit that push the creepy crawly toward or far from the wellspring of vibration and k speaks to the quantity of emphasis. The individual

speaks to the closest creepy crawly to that holds a higher weight, and is the best person. is the vibration that transmitted by the best creepy crawly and comparing weight and position is speak to as pursues:

$$v_{a_2} = W_{a_2} e^{-d_{a_i,2}^2}; W_{a_2} = \max_{k=1,\dots,k} W(a_k) \quad (40)$$

The v_{a_i} is the vibration transmitted by the nearest spider that has the best weight represent as follows:

$$v_{a_1} = W_{a_1} e^{-d_{a_i,1}^2}; W_{a_1} > W_{a_i} \quad (41)$$

In the event that the female concentrates to push toward the wellspring of vibrations, the principal state of condition (5) is utilized, generally the second condition is utilized. The guys creepy crawly update their position dependent on whether male is domineering or non-domineer, where non-domineer arachnids are pulled in toward female's bugs; while the non-domineer insects will in general push toward the focal point of the male populace to progress toward becoming domineer guys. The guys update their situation as pursues:

$$X_{M_{a_i}}^{k+1} = \begin{cases} X_{M_{a_i}}^k + r_1 \times v_{a_3} \times (a_3 - X_{M_{a_i}}^k) + r_3 \times (\xi - 0.5); & W_{M_{a_i}} \geq W_{median} \\ X_{M_{a_i}}^k + r_1 \left(\left(\sum_{a_j=1}^{M_n} X_{M_{a_i}}^k \cdot \frac{W_{a_3+j}}{\sum_{a_j=1}^{M_n} W_{a_3+j}} \right) - X_{M_{a_i}}^k \right); & \text{Otherwise} \end{cases} \quad (42)$$

Where, M_n is the no. of males spider W_{median} is median of weight of all male spider. The weight value of male spider is greater than W_{median} considered as dominant, otherwise, non-dominant. The spider a_3 is the closest female to i^{th} male, and v_{a_3} is the vibrations transmitted by the nearest female and it is defined as:

$$V_{a_3} = W_{a_3} e^{-d_{i,a_3}^2} \quad (43)$$

The final step is mating between the females and dominant male spider on the neighbor with mating radius that defined as follows:

$$M_{F,DM} = \frac{\sum_{a_j=1}^n (X_{a_j}^{high} - X_{a_j}^{low})}{2^n} \quad (44)$$

Be that as it may, maybe there are more than one male and just a single female in this neighbor along these lines, a roulette wheel calculation is utilized to choose the best arrangement. At that point the off springs are created, and the wellness work is processed for them and contrasted and the most exceedingly awful arrangement. The proposed CSSO calculation begins by choosing irregular position for every client (bug), where the number of inhabitants in client is created; at that point position of every client is changed over into a paired vector of length N by the accompanying conditions.

$$TP(X_{a_i}^{a_j}(t)) = \frac{1}{1 + e^{-X_{a_i}^{a_j}(t)}} \quad (45)$$

$$X_{a_i}^{a_j}(t+1) = \begin{cases} 1; & \text{if } TP(X_{a_i}^{a_j}(t)) > [0,1] \\ 0; & \text{Otherwise} \end{cases} \quad (46)$$

where $X_{a_i}^{a_j}(t)$ is the users value at iteration t. For each user a_i , the selected feature is the features that corresponding to 1s and the unselected are corresponding to 0s.

In this paper, the pilot assignment is performed by reuse the pilot sequence for own pilot request from multiple request. The proposed optimization algorithm easily optimizes the time varying channel metrics. The proposed pilot assignment method can offer a powerful way to compute the requested user in the own cell. The fitness function (FF) is an important for proposed CSSO algorithm. We derive the FF based on above discussed multi-factors and expressed as follows:

$$FF = \text{Min}\{R_{ss}, SINR, PEP, NMSE\} \quad (47)$$

Each BS utilizing the condition (38) to register possess pilot flag demand with the client developments. For every client the wellness work is figured and contrasted and the worldwide best wellness. On the off chance that the present estimation of wellness work is better, at that point the is supplanted with and the relating pilot demand turns into the claim solicitation and BS dole out reuse pilot as well. From that point onward, the FF of every client is refreshed by its sort. This procedure is rehashed until the halting basis is fulfilled. The working function of proposed pilot pattern design is summarized in Algorithm 1.

Algorithm 1 Pilot pattern design using CSSO algorithm	
1.	Input: $R_{ss}, \beta, SINR, PEP, NMSE, SR, SEE$
2.	Output: Own pilot signal request
3.	Initialize the number of users, number of antennas, number of iteration (J_{max}) and best fitness function (FF_{best})
4.	Initialize a population of n users: $a_{i_i}; i = 1, 2, \dots, n$
5.	$i=0$
6.	repeat
7.	for all a_{i_i} do
8.	$FF_i = \text{Min}\{R_{ss}, \beta, SINR, PEP, NMSE, SR, SEE\}$
9.	if then ($FF_i < FF_{best}$)
10.	$a_{best} = a_{i_i}, FF_{best} = FF_i$
11.	end if
12.	end for
13.	Compute the worst and best FF using equation (3) and (4).
14.	Compute the weight using equation (2).
15.	Discriminate the own pilot request using equation (5) and (8).
16.	Compute the mating request (between the cell) using equation (10).
17.	$i=i+1$
18.	until $i < J_{max}$

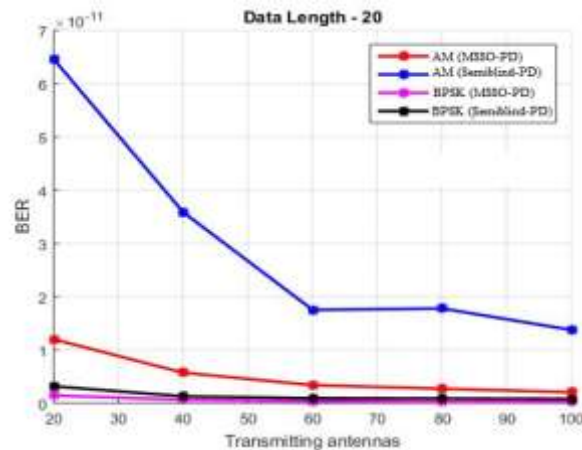
V. Result and Discussion

The performances of proposed Multi-Factor Social Spider Optimization algorithm-based pilot decontamination method are surveyed by performance. The projected pilot decontamination in time-varying channel is executed using MATLAB coding that was replicated in scheme specifications of 4 GB RAM and 3.2 GHz Intel i-5 processor. The evaluation metrics employed are SER, BER, and MMSE. The evaluation metric values are taken under two different scenarios such as varying number of transmitting antennas and varying number of users (receiving nodes).

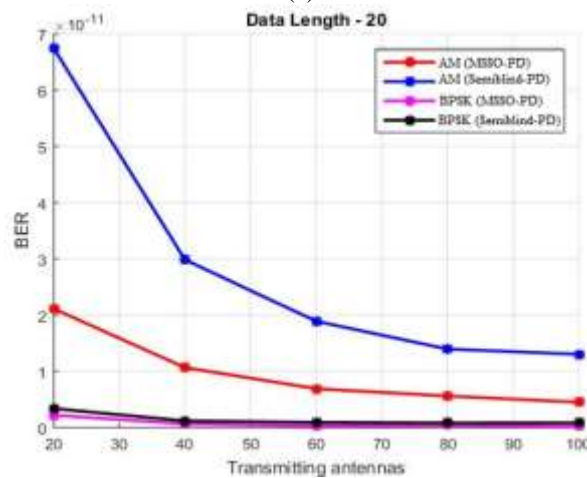
Both adaptive and BPSK modulation are considered in the simulations. The performance of proposed ECE-OA method is compared with the existing semi blind pilot decontamination method.

A. Performance comparison with varying number of transmitting antennas

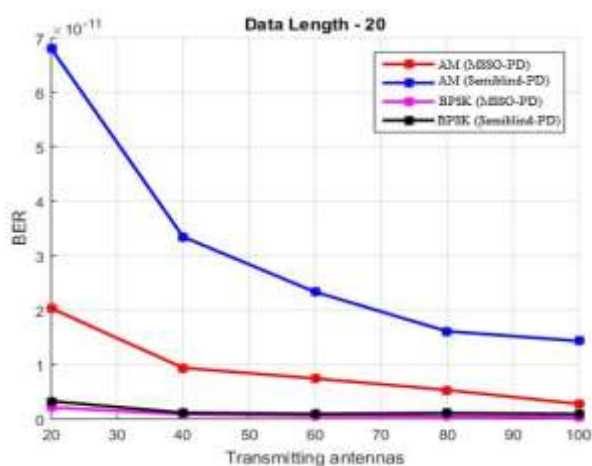
In this section, we evaluate the performance of our proposed method based on BER, SER, and MMSE with the fixed data length as 20. Then the performance is analyzed by varying number of transmitting antennas in BS with fixed number of users. Here, our proposed method is compared with existing PDGSIP and TPDGSIP method [31]. Fig. 6 illustrates the performance of BER with varying number of antennas. Furthermore, in existing method, characterize noise and transmitting performance of the randomly generated signal. Therefore, we have chosen to compare the performance of our proposed method against that one. From the result shown in Fig. 6a-6d with number of users as 250, 500, 750, and 1000 respectively; one can observe that our proposed ECE-OA method one yield the best performance followed by existing semi-blind PD method for both adaptive modulation (AM) and BPSK modulation schemes. Fig. 7 illustrates the performance of SER with varying number of antennas. From the result shown in Fig. 7a-7d with number of users as 250, 500, 750, and 1000 respectively; one can observe that our proposed ECE-OA method one yield the best performance followed by existing PDGSIP and TPDGSIP method. Fig. 8 illustrates the performance of NMSE with varying number of antennas. From the result shown in Fig. 8a-8b with number of users as 250, 500, 750, and 1000 respectively; one can observe that our proposed ECE-OA method one yield the best performance followed by existing PDGSIP and TPDGSIP method.



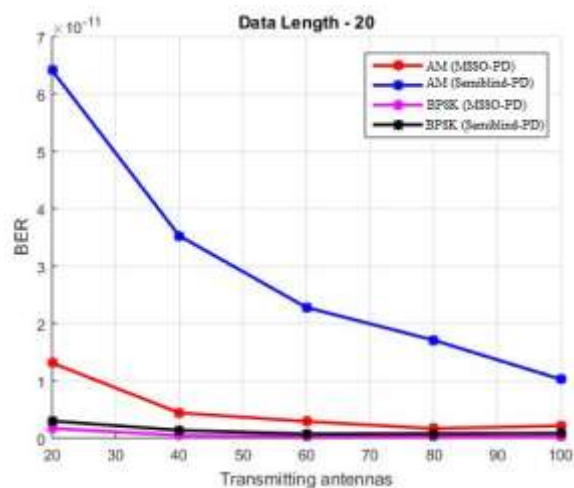
(a)



(b)

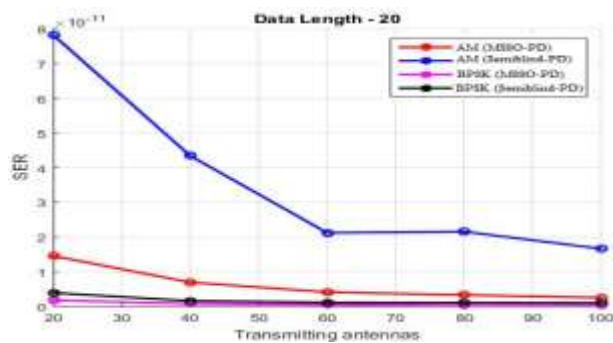


(c)

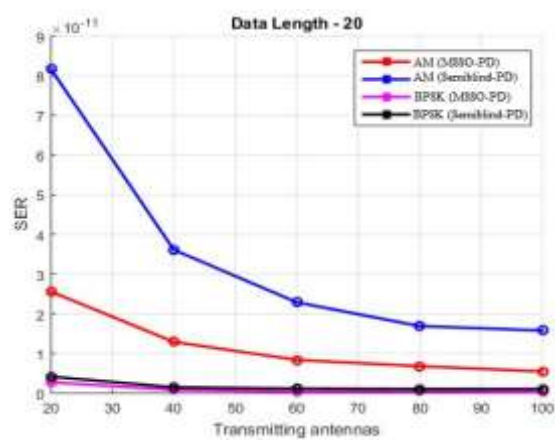


(d)

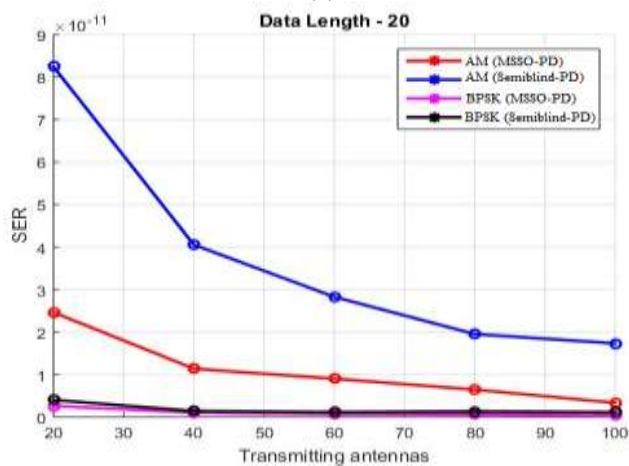
Fig. 6 BER with varying number of antennas with fixed data length as 20 and users as (a) 250 (b) 500 (c) 750 (d) 1000



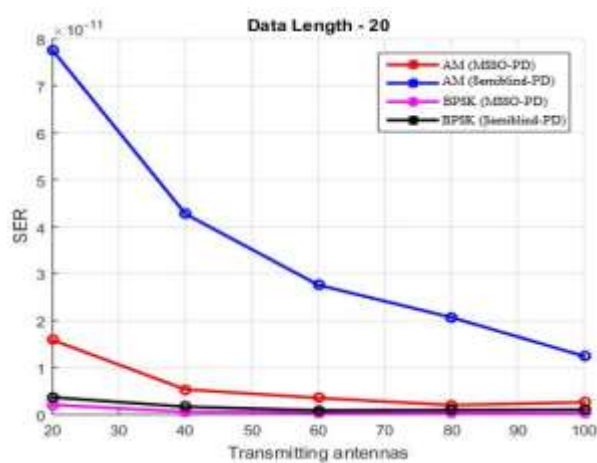
(a)



(b)

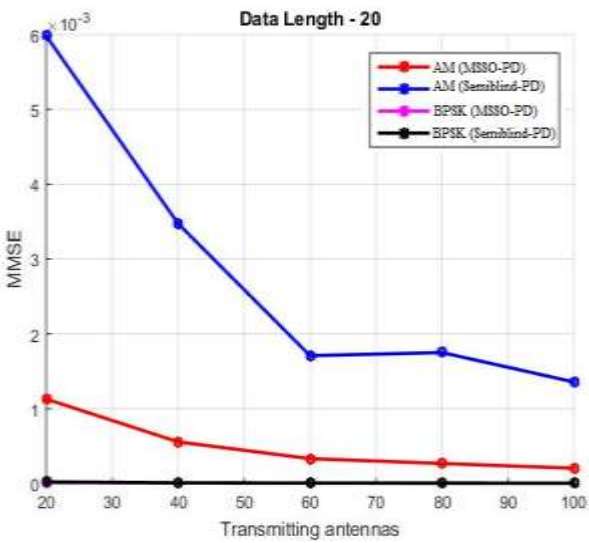


(c)

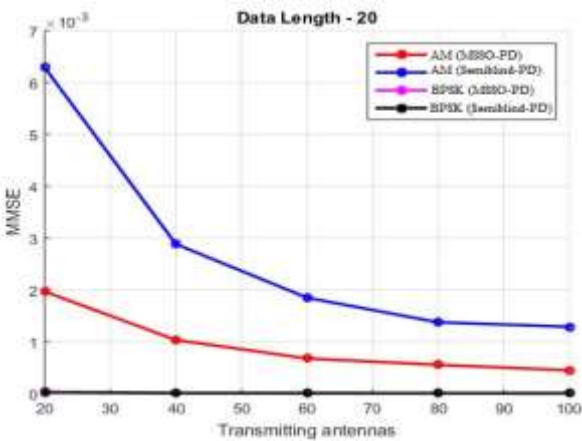


(d)

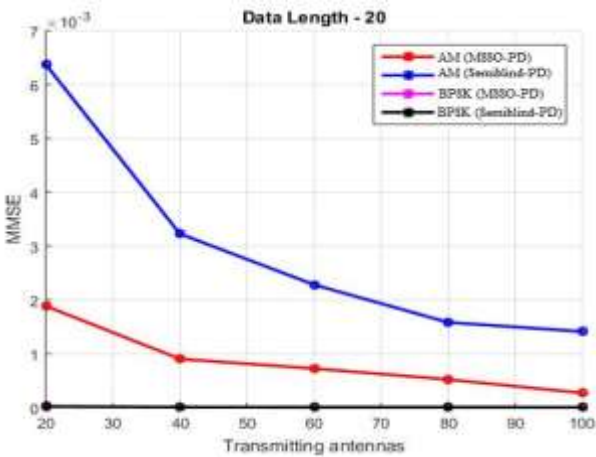
Fig. 7 SER with varying number of antennas with fixed data length as 20 and users as (a) 250 (b) 500 (c) 750 (d) 1000



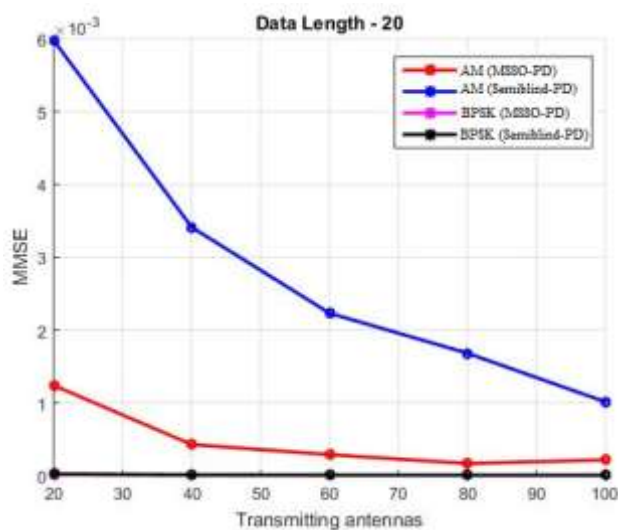
(a)



(b)



(c)



(d)

Fig. 8 NMSE with varying number of antennas with fixed data length as 20 and users as (a) 250 (b) 500 (c) 750 (d) 1000

B. Performance comparison with varying number of users

In this section, we evaluate the performance of our proposed method based on BER, SER, and MMSE with the fixed data length as 20 and fixed number of transmitting antennas as 50. Then the performance is analyzed by varying number of users. Our proposed method is compared with existing PDGSIP and TPDGSIP method. Fig. 9 illustrates the performance of BER with varying number of antennas. From the result shown in Fig. 9 one can observe that our proposed ECE-OA method one yield the best performance followed by existing semi-blind PD method for both adaptive modulation (AM) and BPSK modulation schemes. Fig. 10 illustrates the performance of SER with varying number of users. From the result shown in Fig. 10 one can observe that our proposed ECE-OA method one yield the best performance followed by existing PDGSIP and TPDGSIP method. Fig. 11 illustrates the performance of NMSE with varying number of users. From the result shown in Fig. 11 one can observe that our proposed ECE-OA method one yield the best performance followed by existing PDGSIP and TPDGSIP method.

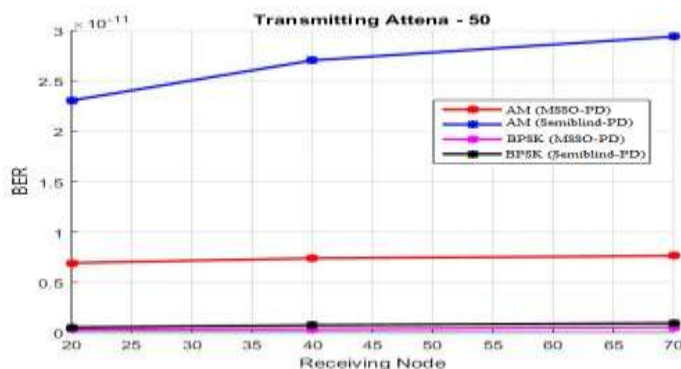


Fig. 9 BER with varying number of users with fixed data length as 20 and antennas as 50

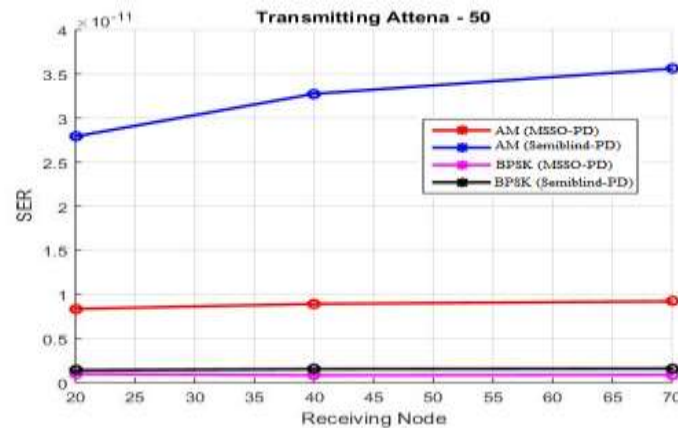


Fig. 10 SER with varying number of users with fixed data length as 20 and antennas as 50

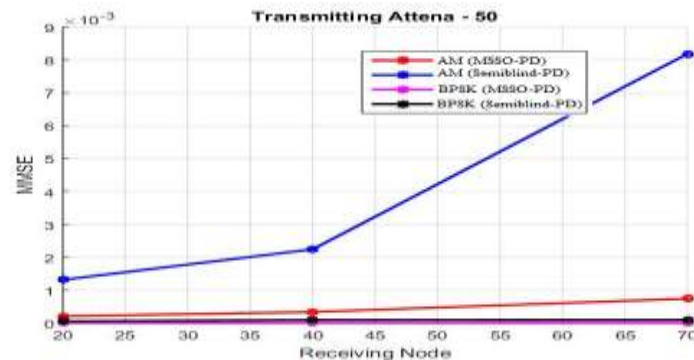


Fig. 11 NMSE with varying number of users with fixed data length as 20 and antennas as 50

VI. Conclusion

We have proposed efficient channel estimation with optimization algorithm based pilot pattern design (ECE-OA) for MIMO-OFDM wireless networks. A chaotic social spider optimization (CSSO) algorithm is used to co-ordinate the assignment of pilot sequences across all cells. The objective of this process is to reduce the correlation between the pilots as observed at each base station. The multiple metrics are obtained from the uplink (UL) channel state information (CSI), during every UL period users in each cell transmit known pilot sequences to the base station in their own cells and the BS estimates uplink CSI. The simulation results proves the performance of proposed ECE-OA design is perform better than existing state-of-art techniques.

References

1. N. Khalid and O. Akan, "Experimental Throughput Analysis of Low-THz MIMO Communication Channel in 5G Wireless Networks", *IEEE Wireless Communications Letters*, vol. 5, no. 6, pp. 616-619, 2016.
2. Z. Qin, M. Zhang, J. Wang and W. Geyi, "Printed eight-element MIMO system for compact and thin 5G mobile handset", *Electronics Letters*, vol. 52, no. 6, pp. 416-418, 2016.
3. I. Pefkianakis, S. Lee and S. Lu, "Towards MIMO-Aware 802.11n Rate Adaptation", *IEEE/ACM Transactions on Networking*, vol. 21, no. 3, pp. 692-705, 2013.
4. J. Choi, S. Choi and K. Lee, "Sounding Node Set and Sounding Interval Determination for IEEE 802.11ac MU-MIMO", *IEEE Transactions on Vehicular Technology*, vol. 65, no. 12, pp. 10069-10074, 2016.
5. A. Panajotovic, F. Riera-Palou and G. Femenias, "Adaptive Uniform Channel Decomposition in MU-MIMO-OFDM: Application to IEEE 802.11ac", *IEEE Transactions on Wireless Communications*, vol. 14, no. 5, pp. 2896-2910, 2015.
6. H. Yu, B. Shim and T. W. Oh, "Iterative inter stream interference cancellation for MIMO HSPA+ system," in *Journal of Communications and Networks*, vol. 14, no. 3, pp. 273-279, June 2012.

7. Z. Charaabi and M. Testard, "Optimized WiMAX MIMO antenna for base station applications with polarization and spatial diversity", *Bell Labs Technical Journal*, vol. 16, no. 1, pp. 217-234, 2011.
8. G. Li, J. Niu, D. Lee, J. Fan and Y. Fu, "Multi-Cell Coordinated Scheduling and MIMO in LTE", *IEEE Communications Surveys & Tutorials*, vol. 16, no. 2, pp. 761-775, 2014.
9. X. Zhang, Y. Zhang, Y. Pan and W. Duan, "Low-Profile Dual-Band Filtering Patch Antenna and Its Application to LTE MIMO System", *IEEE Transactions on Antennas and Propagation*, vol. 65, no. 1, pp. 103-113, 2017.
10. B. Al-Doori and X. Liu, "The Impact of Efficient Transport Blocks Management on the Downlink Power in MIMO Spatial Multiplexing of LTE-A", *IEEE Signal Processing Letters*, vol. 23, no. 12, pp. 1796-1800, 2016.
11. Y. Han, W. Shin and J. Lee, "Projection-based Differential Feedback for FDD Massive MIMO Systems", *IEEE Transactions on Vehicular Technology*, pp. 1-1, 2016.
12. C. Mollen, J. Choi, E. Larsson and R. Heath, "Uplink Performance of Wideband Massive MIMO With One-Bit ADCs", *IEEE Transactions on Wireless Communications*, vol. 16, no. 1, pp. 87-100, 2017.
13. W. C. Lai, Y. T. Liao and T. Y. Hsu, "A Cost-Effective Preamble-Assisted Engine With Skew Calibrator for Frequency-Dependent I/Q Imbalance in 4x4 MIMO-OFDM Modem," in *IEEE Transactions on Circuits and Systems I: Regular Papers*, vol. 60, no. 8, pp. 2199-2212, Aug. 2013.
14. L. Lu, G. Li, A. Swindlehurst, A. Ashikhmin and R. Zhang, "An Overview of Massive MIMO: Benefits and Challenges", *IEEE Journal of Selected Topics in Signal Processing*, vol. 8, no. 5, pp. 742-758, 2014.
15. T. Bogale and L. Le, "Massive MIMO and mmWave for 5G Wireless HetNet: Potential Benefits and Challenges", *IEEE Vehicular Technology Magazine*, vol. 11, no. 1, pp. 64-75, 2016.
16. X. Zhou, B. Maham and A. Hjørungnes, "Pilot Contamination for Active Eavesdropping", *IEEE Transactions on Wireless Communications*, vol. 11, no. 3, pp. 903-907, 2012.
17. J. Zhang, B. Zhang, S. Chen, X. Mu, M. El-Hajjar and L. Hanzo, "Pilot Contamination Elimination for Large-Scale Multiple-Antenna Aided OFDM Systems", *IEEE Journal of Selected Topics in Signal Processing*, vol. 8, no. 5, pp. 759-772, 2014.
18. N. Krishnan, R. Yates and N. Mandayam, "Uplink Linear Receivers for Multi-Cell Multiuser MIMO With Pilot Contamination: Large System Analysis", *IEEE Transactions on Wireless Communications*, vol. 13, no. 8, pp. 4360-4373, 2014.
19. H. Wang, P. Pan, L. Shen and Z. Zhao, "On the Pair-Wise Error Probability of a Multi-Cell MIMO Uplink System With Pilot Contamination", *IEEE Transactions on Wireless Communications*, vol. 13, no. 10, pp. 5797-5811, 2014.
20. T. Vu, T. Vu and T. Quek, "Successive Pilot Contamination Elimination in Multi antenna Multi cell Networks", *IEEE Wireless Communications Letters*, vol. 3, no. 6, pp. 617-620, 2014.
21. J. Cao, D. Wang, J. Li, S. Sun and X. You, "Uplink Sum-Rate Analysis of Massive MIMO System with Pilot Contamination and CSI Delay", *Wireless Personal Communications*, vol. 78, no. 1, pp. 297-312, 2014.
22. Björnson Emil, Hoydis Jakob, and Sanguinetti Luca "Pilot Contamination is Not a Fundamental Asymptotic Limitation in Massive MIMO." *CoRR abs/1611.09152*, 2016.
23. J. Shen, J. Zhang and K. Ben Letaief, "User capacity of pilot-contaminated TDD massive MIMO systems", 2014 *IEEE Global Communications Conference*, 2014.
24. T. Yao and Y. Li, "Pilot contamination reduction by shifted frame structure in massive MIMO TDD wireless system", *Wuhan University Journal of Natural Sciences*, vol. 20, no. 3, pp. 221-228, 2015.
25. T. Nguyen, V. Ha and L. Bao Le, "Resource Allocation Optimization in Multi-User Multi-Cell Massive MIMO Networks Considering Pilot Contamination", *IEEE Access*, vol. 3, pp. 1272-1287, 2015.
26. A. Khansefid and H. Minn, "Achievable Downlink Rates of MRC and ZF Precoders in Massive MIMO With Uplink and Downlink Pilot Contamination", *IEEE Transactions on Communications*, vol. 63, no. 12, pp. 4849-4864, 2015.
27. A. Khansefid and H. Minn, "On Channel Estimation for Massive MIMO With Pilot Contamination", *IEEE Communications Letters*, vol. 19, no. 9, pp. 1660-1663, 2015.
28. J. Shen, J. Zhang and K. Letaief, "Downlink User Capacity of Massive MIMO Under Pilot Contamination", *IEEE Transactions on Wireless Communications*, vol. 14, no. 6, pp. 3183-3193, 2015.
29. X. Zhu, L. Dai and Z. Wang, "Graph Coloring Based Pilot Allocation to Mitigate Pilot Contamination for Multi-Cell Massive MIMO Systems", *IEEE Communications Letters*, vol. 19, no. 10, pp. 1842-1845, 2015.
30. H. Yin, L. Cottatellucci, D. Gesbert, R. Muller and G. He, "Robust Pilot Decontamination Based on Joint Angle and Power Domain Discrimination", *IEEE Transactions on Signal Processing*, vol. 64, no. 11, pp. 2990-3003, 2016.
31. H. Wu, X. Gao and X. You, "Robust Equalizer for Multicell Massive MIMO Uplink With Channel Model Uncertainty", *IEEE Transactions on Vehicular Technology*, vol. 65, no. 5, pp. 3231-3242, 2016.
32. A. Alqahtani, A. Sulyman and A. Alsanie, "Rateless space-time block code for mitigating pilot contamination effects in multi-cell massive MIMO system with lossy links", *IET Communications*, vol. 10, no. 16, pp. 2252-2259, 2016.
33. X. Guo, S. Chen, J. Zhang, X. Mu and L. Hanzo, "Optimal Pilot Design for Pilot Contamination Elimination/Reduction in Large-Scale Multiple-Antenna Aided OFDM Systems", *IEEE Transactions on Wireless Communications*, vol. 15, no. 11, pp. 7229-7243, 2016.
34. D. Hu, L. He and X. Wang, "Semi-Blind Pilot Decontamination for Massive MIMO Systems", *IEEE Transactions on Wireless Communications*, vol. 15, no. 1, pp. 525-536, 2016.
35. J. Yu and V. Li, "A social spider algorithm for global optimization", *Applied Soft Computing*, vol. 30, pp. 614-627, 2015.
36. E. Cuevas, M. Cienfuegos, D. Zaldívar and M. Pérez-Cisneros, "A swarm optimization algorithm inspired in the behavior of the social-spider", *Expert Systems with Applications*, vol. 40, no. 16, pp. 6374-6384, 2013.
37. T. Hatanaka, K. Uosaki and N. Manabe, "Structure identification in Takagi-Sugeno fuzzy modeling", 2002 *IEEE World Congress on Computational Intelligence*. 2002 *IEEE International Conference on Fuzzy Systems*. FUZZ-IEEE'02. Proceedings (Cat. No.02CH37291).

